

Electronic Supplementary Information for Soft Matter

This journal is © The Royal Society of Chemistry

Supplementary Information

DNA Fragmentation in complicated flow fields created by micro-funnel shapes

Shuyi Wu ^a, Tengfei Fu ^a, Renhui Qiu ^a, Luping Xu ^{b,*}

^a *College of Transportation and Civil Engineering, Fujian Agriculture and Forestry University, Fuzhou,
350108, China.*

^b *Center for Nano and Micro Mechanics, School of Aerospace Engineering, Tsinghua University, Beijing,
100084, China.*

* Corresponding author.

E-mail: lupingxu@tsinghua.edu.cn

Numerical simulation method

The dynamical behavior of DNA molecules was simulated by a BD-CFD method. This method had been introduced in our previous study.¹ Here, we would like to quote and improve the expression of this simulation method. The method includes the simulation of DNA conformational evolution by the Brownian dynamics-computational fluid dynamics (BD) method and the calculation of flow fields by the computational fluid dynamics (CFD) method. After calculating the flow fields in micro-funnels, the flow velocity was imported into the Brownian dynamics equation. The DNA molecules are simulated using a bead-spring model, which contains beads connected by springs. Different types of force, including the flow force, the Brownian force, the spring force, and the excluded volume force, act on the beads and cause the change in conformation of DNA molecules. The parameters in the model are adapted from the mechanical properties of DNA molecules reported in previous experimental and numerical studies.²⁻¹¹

The evolution of velocity and location of the i -th bead of a DNA molecule in flow fields is obtained from the Brownian dynamics equation:

$$\frac{d\mathbf{r}_i}{dt} = \mathbf{V}(\mathbf{r}_i) + \frac{1}{\xi} [\mathbf{F}_i^B(t) + \mathbf{F}_i^S(t) + \mathbf{F}_i^{EV}(t) + \mathbf{F}_i^{EV,wall}(t)], \quad (1)$$

where \mathbf{r}_i is the location of the i -th bead of the DNA, $\mathbf{V}(\mathbf{r}_i)$ is the velocity of the flow field at \mathbf{r}_i , ξ is the drag coefficient of a bead. $\mathbf{F}_i^B(t)$, $\mathbf{F}_i^S(t)$, \mathbf{F}_i^{EV} and $\mathbf{F}_i^{EV,wall}$ are the Brownian force, total spring force acting on the bead, sum of the excluded volume force from other beads and excluded volume force between the

bead and the wall, respectively. We nondimensionalize Eq. (1) using the following dimensionless parameters to facilitate the simulation:

$$\hat{\mathbf{r}} \equiv \frac{\mathbf{r}}{l}, \hat{t} \equiv \frac{t}{\xi l^2 / k_B T}, \hat{\mathbf{V}} \equiv \frac{\mathbf{V}}{V_0}, \hat{\mathbf{F}}(\hat{\mathbf{r}}) \equiv \frac{\mathbf{F}(\mathbf{r})}{k_B T / l}, \quad (2)$$

where l is the contour length of a DNA segment that is represented by a bead, $k_B T$ is the thermal energy, and V_0 is the average velocity in the moving direction at the inlet. Accordingly, the dimensionless Brownian dynamic equation is

$$\frac{d\hat{\mathbf{r}}_i}{d\hat{t}} = Pe \hat{\mathbf{V}}(\hat{\mathbf{r}}_i) + \hat{\mathbf{F}}_i^B + \hat{\mathbf{F}}_i^S + \hat{\mathbf{F}}_i^{EV} + \hat{\mathbf{F}}_i^{EV,wall}, \quad (3)$$

where $Pe = V_0 l / D$ is the Peclet number of a bead, and $D = k_B T / \xi$ is the diffusivity of a bead.

$\hat{\mathbf{F}}_i^B$ is the dimensionless Brownian force at a bead that is described by

$$\hat{\mathbf{F}}_i^B = \sqrt{\frac{6}{\Delta \hat{t}}} \mathbf{n}_i, \quad (4)$$

where \mathbf{n}_i is a vector and each of its components is uniformly distributed between -1 and 1.¹²

Based on previous studies and experimental results,^{2-11, 13} the spring force from the i -th bead to the $(i + 1)$ -th bead, $\hat{f}_{i,i+1}^S$, was described by a piecewise function for different stages of the stress-strain relationship of DNA as follows:

$$\hat{f}_{i,i+1}^S = \left\{ \begin{array}{l} \frac{1}{A_p^{\text{eff}}} \left\{ \hat{r}_{i+1,i} - \frac{1}{4} + \frac{1}{4(1-\hat{r}_{i+1,i})^2} \right\} \frac{\hat{r}_{i+1,i} - \hat{r}_i}{\hat{r}_{i+1,i}}, \quad SR < 0.95 \\ \hat{f}_{i,i+1}^S(SR|_{0.95}) + \frac{k_1 \times (SR - 0.95)}{k_B T / l}, \quad 0.95 \leq SR < 1.1 \\ \hat{f}_{i,i+1}^S(SR|_{1.1}), \quad 1.1 \leq SR < 1.7 \\ \hat{f}_{i,i+1}^S(SR|_{1.7}) + \frac{k_2 \times (SR - 1.7)}{k_B T / l}, \quad 1.7 \leq SR < 2.14 \end{array} \right\}. \quad (5)$$

where $\hat{r}_{i+1,i}$ is the dimensionless distance between the i -th bead and the $(i+1)$ -th bead and SR stands for stretching ratio. The variables k_1 and k_2 are the slopes of the linear stages in the stress-strain relationship of B-form and S-form DNA, respectively. A_p^{eff} is the effective persistence length, which is higher than the true persistence length of DNA A_p (0.053 μm) to compensate for the artificially induced additional flexibility caused by the discretization of the beads-springs model.¹² For the bead-spring model of λ DNA with a different number of beads N_b , A_p^{eff} was set according to an empirical relationship between A_p^{eff} and N_b .¹⁴ Then, the total spring force acting on the i -th bead can be calculated as

$$\hat{\mathbf{F}}_i^S = \begin{cases} \hat{\mathbf{f}}_{i,i+1}^S, & i = 1 \\ \hat{\mathbf{f}}_{i,i+1}^S + \hat{\mathbf{f}}_{i,i-1}^S, & 1 < i < N_b \\ \hat{\mathbf{f}}_{i,i-1}^S, & i = N_b \end{cases} \quad (6)$$

$\hat{\mathbf{F}}_i^{EV}$ is the dimensionless excluded volume force acting on the i -th bead from other beads, which is determined as follows:

$$\hat{\mathbf{F}}_i^{EV} = - \sum_{j=1(j \neq i)}^{N_b} \frac{9}{2} \hat{v}^{EV,P} \left(\frac{3}{4\sqrt{\pi}} \right)^3 \lambda^{\frac{9}{2}} \exp\left(\frac{-9\lambda \hat{r}_{ji}^2}{4} \right) \hat{\mathbf{r}}_{ji}, \quad (7)$$

where $\hat{v}^{EV,P} = v^{EV,P}/l^3$ is the dimensionless excluded volume parameter $v^{EV,P}$, and the segment number λ is l/A_p .¹²

The bead-wall interaction includes a repulsive potential and a repositioning process. When a bead in the fluid is too close to the boundary of the microfluidic channel, the bead will be prevented from penetrating the wall by a repulsive potential:^{12, 15}

$$U_i^{wall} = \frac{A_{wall}}{6A_p\delta_{wall}^2} (d - \delta_{wall})^3, \quad (8)$$

where $A_{wall} = 25 k_B T$ is the energy barrier, and $\delta_{wall} = A_p \sqrt{\lambda/2}$ is the cut-off distance. The variable d is the distance between the i -th bead and the wall. When a bead penetrates the wall of the device, this bead will be re-positioned to the nearest wall via the modified Heyes-Melrose algorithm:^{16, 17}

$$\Delta \hat{\mathbf{r}}_i^{rp} = \Delta \hat{\mathbf{P}}_i H(\Delta \hat{p}_i), \quad (9)$$

where $\Delta \hat{\mathbf{r}}_i^{rp}$ is the dimensionless repositioning vector for the penetrated bead. $\Delta \hat{\mathbf{P}}_i$ is the dimensionless distance vector from the penetrated bead to the nearest wall, and $\Delta \hat{p}_i$ is the magnitude of $\Delta \hat{\mathbf{P}}_i$. H is the Heaviside step function.

In this work, we ignore the reaction from DNA to flow field and the effect of hydrodynamic interaction (HI) between beads and walls. HI effect should be considered when DNA's contour length is larger than 150 μm .¹⁸ For λ DNA with a contour length about 17 μm and its even shorter fragments, hydrodynamic simulations with or without HI show negligible difference.¹⁹⁻²¹ In previous studies, the BD-CFD method without considering the effect of HI has been used to simulate the stretching behavior of DNA molecules in microfluidic chips and to guide the design of microfluidic devices.^{12, 16, 22}

In order to set the simulation time step, we calculate the local velocities of the flow field at locations of all beads in a DNA molecules, $v(\mathbf{r}_i)$. The simulation step time is set as $t_{step} = 10^{-8} / \max(v(\mathbf{r}_i))$ (s), where the $\max(v(\mathbf{r}_i))$ is the maximum local velocity of the flow field.

A DNA molecule will be broken when stretching force acting on the molecule is larger than its tensile strength. In this study, we use this tensile strength and the corresponding critical stretching ratio as the criterion of fragmentation. Some reported studies measured the mechanical properties of single DNA molecule using optical tweezers, magnetic tweezers, atomic force microscope (AFM) and molecular combing^{3-9, 11}. According to the experimental data, we set the tensile strength of DNA molecules in our simulation as 483 pN and the corresponding critical stretching ratio as 2.14, the former of which is almost the average of reported data.

Although the differences in base sequence can cause the variation of strength along DNA chains, we ignored the effect of the strength variation on DNA fragmentation based on the following information. First, the difference of base-pair unbinding force (about 10 pN)²³ is much smaller than the breaking strength of phosphodiester bonds (over 600 pN)¹⁰ on the DNA backbone. And experiments showed that the breaking strengths between poly(dT) and poly(dA) are similar.⁸ Second, in the numerical simulations of this study, one bead of the DNA model stands for a DNA segment of 1.6 kbp, which is long enough to ignore the variation of DNA strength caused by the differences in base sequence. Third, previous experimental studies showed that the fragmentation locations along DNA molecules are fairly random.^{24, 25}

Effect of DNA length on fluorescence intensity

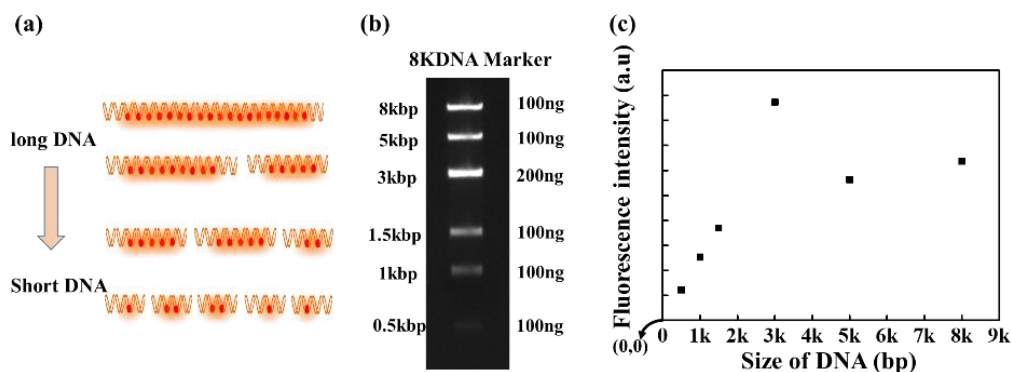


Figure S1 Relation between the length of DNA molecules and fluorescence intensity.

(a) A schematic for the effect of DNA length on fluorescence intensity, indicating that shorter DNA molecules produce weaker fluorescence intensity. The double-helical lines represent DNA molecules and the orange dots signify fluorescent molecules combined with DNA. (b) The electrophoresis image of the 8K DNA marker including DNA pieces of 8 kbp, 5 kbp, 3 kbp, 1.5 kbp, 1 kbp, and 0.5 kbp. (c) The fluorescence intensity versus the size of DNA molecules.

Micro-funnel with a constant extension rate

Table 1 Description of the micro-funnel

Name	Feature	Shape function
Funnel 5	Constant extension rate	$w(x) = \frac{w_{in}}{1 + x(w_{in}/w_{out} - 1)/l_f}$

Parameters description: The $w(x)$ is the channel width where the abscissa is x ; the $w_{in} = 200 \mu\text{m}$ is half of the width of funnel entrance; the $w_{out} = 15 \mu\text{m}$ is half of the width of funnel exit; the $l_f = 200 \mu\text{m}$ is the funnel length.

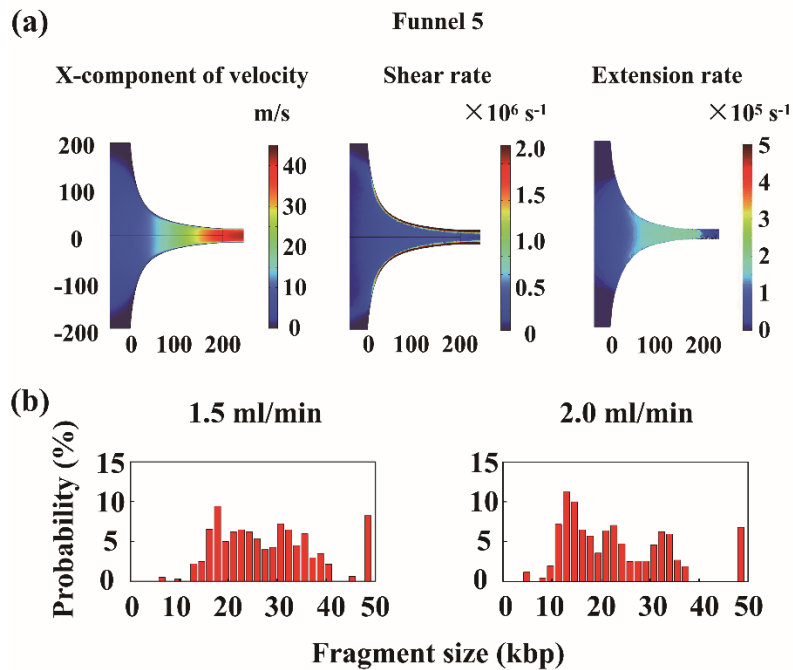


Figure S2 The flow field and fragmentation performance for the micro-funnel with a constant extension rate (Funnel 5). (a) The x-component of velocity, the shear rate, and the extension rate of the flow field at a flow rate of 3 ml/min. (b) The fragment size distributions of produced DNA pieces with flow rates of 1.5 ml/min and 2 ml/min from numerical simulations.

References

1. S. Wu, C. Li, Q. Zheng and L. Xu, *Soft Matter*, 2018, **14**, 8780-8791.
2. A. Bensimon, A. Simon, A. Chiffaudel, V. Croquette, F. Heslot and D. Bensimon, *Science*, 1994, **265**, 2096-2098.
3. D. Bensimon, A. J. Simon, V. V. Croquette and A. Bensimon, *Phys Rev Lett*, 1995, **74**, 4754-4757.
4. C. P. Calderon, W. H. Chen, K. J. Lin, N. C. Harris and C. H. Kiang, *J Phys Condens Matter*, 2009, **21**, 34114.
5. W. S. Chen, W. H. Chen, Z. Chen, A. A. Gooding, K. J. Lin and C. H. Kiang, *Phys Rev Lett*, 2010, **105**, 218104.
6. P. Cluzel, A. Lebrun, C. Heller, R. Lavery, J. L. Viovy, D. Chatenay and F. Caron, *Science*, 1996, **271**, 792-794.
7. V. S. Jadhav, D. Bruggemann, F. Wruck and M. Hegner, *Beilstein J Nanotechnol*, 2016, **7**, 138-148.
8. C. Ke, M. Humeniuk, S. G. H and P. E. Marszalek, *Phys Rev Lett*, 2007, **99**, 018302.
9. R. Krautbauer, L. H. Pope, T. E. Schrader, S. Allen and H. E. Gaub, *FEBS Lett*, 2002, **510**, 154-158.
10. J. Li, S. S. Wijeratne, X. Qiu and C. H. Kiang, *Nanomaterials (Basel)*, 2015, **5**, 246-267.
11. M. Rief, H. Clausen-Schaumann and H. E. Gaub, *Nature Structural Biology*, 1999, **6**, 346-349.

12. C. D. Huang, D. Y. Kang and C. C. Hsieh, *Biomicrofluidics*, 2014, **8**, 014106.
13. A. A. Almqwashi, T. Paramanathan, I. Rouzina and M. C. Williams, *Nucleic Acids Res*, 2016, **44**, 3971-3988.
14. W. C. Liao, X. Hu, W. Wang and L. James Lee, *Biomicrofluidics*, 2013, **7**, 34103.
15. R. M. Jendrejack, D. C. Schwartz, M. D. Graham and J. J. de Pablo, *Journal of Chemical Physics*, 2003, **119**, 1165-1173.
16. C. C. Hsieh and T. H. Lin, *Biomicrofluidics*, 2011, **5**, 44106-4410617.
17. J. M. Kim and P. S. Doyle, *J Chem Phys*, 2006, **125**, 074906.
18. C. M. Schroeder, E. S. G. Shaqfeh and S. Chu, *Macromolecules*, 2004, **37**, 9242-9256.
19. R. M. Jendrejack, J. J. de Pablo and M. D. Graham, *The Journal of Chemical Physics*, 2002, **116**, 7752-7759.
20. C.-C. Hsieh, L. Li and R. G. Larson, *Journal of Non-Newtonian Fluid Mechanics*, 2003, **113**, 147-191.
21. P. T. Underhill and P. S. Doyle, *Journal of Non-Newtonian Fluid Mechanics*, 2007, **145**, 109-123.
22. D. W. Trahan and P. S. Doyle, *Biomicrofluidics*, 2009, **3**, 12803.
23. M. Rief, H. Clausen-Schaumann and H. E. Gaub, *Nat Struct Biol*, 1999, **6**, 346-349.
24. I. V. Nesterova, M. L. Hupert, M. A. Witek and S. A. Soper, *Lab Chip*, 2012, **12**, 1044-1047.
25. P. Oefner, *Nucleic Acids Res*, 1996, **24**, 3879-3886.